

**Nanoscopic interferometer model for spin resonance in current noise**

Anatoly Golub and Baruch Horovitz

*Department of Physics, Ben-Gurion University of the Negev, Beer-Sheva, Israel*

(Received 4 June 2013; revised manuscript received 29 July 2013; published 17 September 2013)

We study a model for the observed phenomenon of electron spin resonance (ESR) at the Zeeman frequency as seen by a scanning tunneling microscope (STM) via its current noise. The model for this ESR-STM phenomenon allows the STM current to flow in two arms of a nanoscopic interferometer, one arm has direct tunneling from the tip to the substrate while the second arm has tunneling through two spin states. We evaluate analytically the noise spectrum for nonpolarized leads, as relevant to the experimental setup. We show that spin-orbit interactions allow for an interference of two tunneling paths resulting in a resonance effect.

DOI: [10.1103/PhysRevB.88.115423](https://doi.org/10.1103/PhysRevB.88.115423)

PACS number(s): 73.63.-b, 74.55.+v, 73.63.Kv, 73.50.Td

**I. INTRODUCTION**

The control and detection of single spins is of considerable recent interest. A particularly interesting method of detecting a single spin on a surface is possible by a scanning tunneling microscope (STM).<sup>1</sup> The technique has been initiated and developed by Manassen and various collaborators.<sup>1-4</sup> It is based on monitoring the noise, i.e., the STM current-current correlations, and observing a signal at the expected Larmor frequency, a signal that is sharp even at room temperature. The Larmor frequency is also seen in an electron spin resonance (ESR) experiment with many spins; in contrast, the ESR-STM method observes a single spin and furthermore, the system is static, no oscillating field is applied as in ESR. The observed frequency is found to vary linearly with the applied magnetic field, confirming that the STM has detected an isolated spin on the surface. This phenomenon was first demonstrated on oxidized Si(111) surface<sup>2,3</sup> and then on Fe atoms<sup>4</sup> on Si(111) as well as on a variety of organic molecules on a graphite surface<sup>5</sup> and on Au(111) surfaces.<sup>6-8</sup> Recent extensions have resolved two resonance peaks on an oxidized Si(111)  $7 \times 7$  surface corresponding to site specific  $g$  factors<sup>9,10</sup> as well as to observation of hyperfine coupling.<sup>1</sup> We further note that the spatial dependence of the signal shows a nonmonotonic contour plot, i.e., the signal is elongated and is maximal at  $\sim 1$  nm on either side of a minimum point.<sup>2,3</sup>

The theoretical understanding of the ESR-STM effect is not settled.<sup>1</sup> The emergence of a finite frequency in a steady state stationary situation is a nontrivial phenomenon. An obvious mechanism for coupling the charge current to the spin precession is spin-orbit coupling.<sup>11</sup> It was shown that an ESR signal is present in the noise with spin-orbit coupling when the leads are polarized, either for a strong Coulomb interaction<sup>12-14</sup> or for the noninteracting case,<sup>13</sup> and even in linear response.<sup>15</sup> However, the experimental data<sup>1</sup> involves a small field of  $\sim 200$  G corresponding to a Larmor frequency of  $\sim 500$  MHz, i.e.,  $\sim 10^{-7}$  relative to a lead's bandwidth. It was found in these spin-orbit models<sup>12-14</sup> that the signal vanishes when the lead polarization vanishes, or when the lead and dot polarization are parallel, as for a uniform magnetic field. It was argued that an effective spin polarization is realized as a fluctuation effect either for a small number of electrons that pass the localized spin in one cycle<sup>16</sup> or due to  $1/f$  magnetic noise of the tunneling current.<sup>17</sup> It was further shown that spin-orbit coupling in an asymmetric dot

can yield an oscillating electric dipole, possibly affecting the STM current.<sup>18</sup>

In the present paper we follow a recently proposed model that allows for an ESR-STM phenomena with nonpolarized leads.<sup>19</sup> The model assumes an additional direct tunneling between the tip and the substrate in parallel to tunneling via the dot's states, i.e., a nanoscopic interferometer. The numerical study<sup>19</sup> shows that the interference of the direct current and that via the spin has an ESR signal in the noise, a signal that increases with the direct tunneling. This model is motivated by studies of quantum dots with spin orbit<sup>20</sup> and by STM studies of a two-impurity Kondo system that shows a significant direct coupling between the tip and substrate states.<sup>21</sup> Similar models including an Aharonov-Bohm phase have been studied.<sup>22-25</sup> The nanoscopic interferometer model is consistent with the unusual nonmonotonic contour plot,<sup>2,3</sup> i.e., the signal is maximized when the STM tip is not directly on the spin center but slightly away, so as to maximize an overlap with a surface state of the substrate. In the present work we consider nonpolarized leads, as relevant to the experimental setup, and evaluate the noise analytically in the stationary system, in accordance with the numerical results for this case. The analytic results clarify the physical processes of the resonance phenomenon and allow us to discuss the ESR-STM effect for a broad range of parameters. As detailed in the conclusion section, the present work allows for a full analysis of the parameters of the experiment and for predictions on the signal intensity as a function of various parameters.

The paper is organized as follows. In Sec. II we introduce the Hamiltonian of the system and present the results for direct tunneling: effective action, the current, and the current noise power spectrum. Section III contains the effective action of the dot and the expression for the current flow through the dot. Section IV reflects our principal result: the resonance part of the current spectral density. The results are illustrated by Figs. 1 and 2. Finally our conclusions are contained in Sec. V. The Appendices A, B, and C give various details of the calculations.

**II. HAMILTONIAN**

The Hamiltonian of the system describes direct tunneling through the dot between left (L) and right (R) leads as well as L-R tunneling via the dot states,

$$H = H_L + H_R + H_D + H_W + H_T, \quad (1)$$

where the lead Hamiltonians are  $H_l = \sum_{l,k,\sigma} \epsilon_{l,k} c_{l,k,\sigma}^\dagger c_{l,k,\sigma}$ ,  $l = L, R$ ,  $\sigma = \pm$  is the spin, and  $k$  are the continuum states. The dot Hamiltonian is  $H_D = \sum_{\sigma} \epsilon_{\sigma} d_{\sigma}^{\dagger} d_{\sigma}$  with  $\epsilon_{\sigma} = \epsilon_0 + \sigma H$ ,  $\epsilon_0$  is the mean position of the dot levels, and  $H$  is the applied magnetic field that includes the  $g$  factor and the Bohr magneton. We assume that the dispersions  $\epsilon_{l,k}$  of the lead electrons are spin independent, justified by the small ratio  $\sim 10^{-7}$  of the Larmor frequency and a typical electron bandwidth.

A general spin-orbit coupling involves unitary matrices that can be parameterized<sup>19</sup> by two angles  $\phi, \theta$ . The angle  $\phi$  appears in the Hamiltonian for the direct tunneling

$$H_W = W \sum_{k,\sigma} e^{i\sigma\phi} c_{L,k,\sigma}^\dagger c_{R,k,\sigma} + \text{H.c.} \quad (2)$$

The spin dependent form in  $e^{i\sigma\phi}$  is required by time reversal. The angle  $\theta$  appears in the tunneling via the dot as a spin rotation in the  $R$  lead, while the  $L$  lead is diagonal in spin

$$H_T = t \sum_{k,\sigma} [c_{L,k,\sigma}^\dagger d_{\sigma} + c_{R,k,\sigma}^\dagger U_{\sigma,\sigma'} d_{\sigma'}] + \text{H.c.}, \quad (3)$$

where

$$U = \begin{pmatrix} \cos(\theta/2) & \sin(\theta/2) \\ \sin(-\theta/2) & \cos(\theta/2) \end{pmatrix}. \quad (4)$$

We note that special cases of this parametrization have been used in related models.<sup>13,22,23</sup>

To calculate the current and the noise, we use the Keldysh formalism<sup>26,27</sup> and include in the action a quantum source field  $\hat{\alpha}$  that couples to the total current. The source term has the form  $\hat{\alpha} = \frac{1}{2}\alpha\sigma_x$  where  $\sigma_x$  is a Pauli matrix in the rotated Keldysh space. The total action is  $S_{\text{tot}} = S_T + S_D + S_W$ , where  $S_T$  corresponds to  $H_T$ , i.e., tunneling via the dot

$$S_T = -t \int dt \{ c_{L,\sigma}^\dagger(0)(1 - \hat{\alpha}/2)d_{\sigma} + c_{R,\sigma}^\dagger(0)(1 + \hat{\alpha}/2)U_{\sigma,\sigma'}d_{\sigma'} + \text{H.c.} \} \quad (5)$$

and  $S_D$  is the action of the dot

$$S_D = \int dt d^\dagger G_0^{-1} d. \quad (6)$$

$G_0$  is the Green's function (GF) of the noninteracting dot in the rotated Keldysh representation that has the form

$$G_0 = \begin{pmatrix} G_0^R & G_0^K \\ 0 & G_0^A \end{pmatrix}, \quad (7)$$

with retarded ( $R$ ), advanced ( $A$ ), and Keldysh ( $K$ ) indices as superscripts. The current via the dot  $\delta S_T / \delta \alpha$  is chosen as a symmetric combination of the current from the left lead to the dot  $J_{L \rightarrow d}$  and that from the dot to the right lead  $J_{d \rightarrow R}$ . In general a linear combination of these currents is needed, depending on various capacitances.<sup>28</sup> We expect that the resonance effect is dominated by single occupancy of the dot and the latter two currents are equal. Indeed we check below that our results for the resonance term do not depend on which linear combination is used. Furthermore, the numerical study<sup>19</sup> used  $J_{L \rightarrow d}$  for the noise evaluation with results consistent with our analytic ones.

Here and below the dot electron operator  $d$  becomes a vector in spin space (and Keldysh space). The GF  $G_0^{R,A,K}$  are diagonal in spin space and in terms of a Fourier energy variable  $\epsilon$  are given by

$$\begin{aligned} G_{0,\sigma}^R(\epsilon) &= \frac{1}{\epsilon - \epsilon_0 - \sigma H + i\delta} \\ G_{0,\sigma}^A(\epsilon) &= \frac{1}{\epsilon - \epsilon_0 - \sigma H - i\delta} \\ G_{0,\sigma}^K(\epsilon) &= -2\pi i \tanh\left(\frac{\epsilon}{2T}\right) \delta(\epsilon - \epsilon_0 - \sigma H) \end{aligned} \quad (8)$$

with the limit  $\delta = +0$ .

The part of the action  $S_W$  which contains the leads and the direct LR tunneling is

$$\begin{aligned} S_W &= \int dt \sum_{k,k'} c_{k\sigma}^\dagger g_{kk'\sigma}^{-1} c_{k'\sigma} \\ g_{kk'\sigma}^{-1} &= g_{k\sigma}^{-1} \delta_{kk'} - W [e^{i\phi\sigma} A_{kk'} \rho_+ (1 + \hat{\alpha}) \\ &\quad + e^{-i\phi\sigma} A_{kk'} \rho_- (1 - \hat{\alpha})]. \end{aligned} \quad (9)$$

Here  $c_{k\sigma}$ ,  $\rho_{\pm} = (\rho_x \pm i\rho_y)/2$  are vectors and Pauli matrices, respectively, in LR (left-right) space, the GFs of the leads  $g_{k\sigma}^{-1}$  are diagonal in LR space, and  $A_{kk'} = 1$  present a constant matrix in momentum  $k, k'$  space. Fermion operators and GF as well the quantum source field  $\hat{\alpha} = \alpha\sigma_x$  acts in the rotated Keldysh space. The voltage  $V$  between the leads is assumed small relative to the bandwidths, hence the density of states  $N_R, N_L$  are taken as constants. The GF  $g_{k\sigma}$  has the structure of Eq. (7) and its momentum integrated forms  $\bar{g}_l^{R,A,K} = \sum_k g_{l,k}^{R,A,K} / (2\pi N_l)$  are

$$\begin{aligned} \bar{g}^R &= \frac{1}{2\pi N_l} \sum_k \frac{1}{\epsilon - \epsilon_{l,k} + i\delta} = -\frac{1}{2} i \\ \bar{g}^A &= \frac{1}{2\pi N_l} \sum_k \frac{1}{\epsilon - \epsilon_{l,k} - i\delta} = +\frac{1}{2} i \\ \bar{g}_{R,L}^K(\epsilon) &= -i f_{R,L}(\epsilon), \end{aligned} \quad (10)$$

where  $V$  is the voltage difference between the LR leads and  $f_{R,L}(\epsilon) = \tanh \frac{\epsilon \mp V/2}{2T}$ .

To cope with scattering of electrons due to the tunneling we shift the operators  $c_{k\sigma}$  so as to cancel the linear coupling to  $d_{\sigma}$  in Eq. (5). This adds a term of the form  $d^\dagger Q(\alpha)d$  to the dot action and then the effective action separates into two independent parts  $S_{\text{tot}} = S_W + S_{\text{dot}}$ . The total generating functional  $Z_{\text{tot}}(\alpha)$ , as a function of the source field, is therefore factorized into  $Z_{\text{tot}} = Z_W Z_{\text{dot}}$ .

We consider now the  $S_W$  part of the effective action. Inverting  $g^{-1}$  by using blockwise matrix inversion we obtain

$$\begin{aligned} g_{LLkk'} &= g_{Lk} \delta_{kk'} + g_{Lk} x_L D_L^{-1} g_{Lk'} \\ g_{RRkk'} &= g_{Rk} \delta_{kk'} + g_{Rk} x_R D_R^{-1} g_{Rk'}. \end{aligned} \quad (11)$$

Here  $D_{L,R} = 1 - 4x \bar{g}_{L,R}(1 \pm \hat{\alpha}) \bar{g}_{R,L}(1 \mp \hat{\alpha})$ ,  $x_{L,R} = 2\pi N_{R,L} W^2 (1 \pm \hat{\alpha}) \bar{g}_{R,L}(1 \mp \hat{\alpha})$ , and the coupling parameter

$$x = \pi^2 N_L N_R W^2. \quad (12)$$

The electron transport and noise calculations involve only the integrated GF of Eq. (10).

Direct integration over electron operators  $c_{l,k,\sigma}$  yields  $Z_W = \det[g^{-1}] = \exp[\text{Tr} \ln g^{-1}]$ . The direct current  $J_W$  and related noise power are defined as derivatives with respect to the source field (taking  $\alpha = 0$  after derivatives is implied)

$$J_W(t) = \frac{\delta \ln Z_W}{\delta \alpha(t)} = \frac{\delta \text{Tr} \ln(g^{-1})}{\delta \alpha(t)} \quad (13)$$

$$S_W = \frac{\delta^2 \ln Z_W}{\delta \alpha(t) \delta \alpha(t')}. \quad (14)$$

We obtain the textbook results<sup>28</sup> for noise and transport current through a contact with transmission probability<sup>22</sup>  $T_B = 4x/(1+x)^2$  and reflection coefficient  $R_B = 1 - T_B$  (details in Appendix A); the conductance is then  $\frac{2e^2}{h} T_B$ .

### III. EFFECTIVE ACTION

The effective action of the dot includes the  $Q(\alpha)$  term from the integration over the lead fermions. It is expressed (in Keldysh space) in terms of various GFs  $\hat{g}_{ll'}$  as listed in Eq. (A1) and in terms of the noninteracting dot GF Eq. (7) as

$$S_{\text{dot}} = \int dt d^\dagger G^{-1} d \quad (15)$$

$$\begin{aligned} G^{-1} &= G_0^{-1} - Q(\alpha) \\ Q(\alpha) &= \Gamma_L \left(1 - \frac{\hat{\alpha}}{2}\right) \hat{g}_{LL} \left(1 + \frac{\hat{\alpha}}{2}\right) \\ &+ \Gamma_R \left(1 + \frac{\hat{\alpha}}{2}\right) \hat{g}_{RR} \left(1 - \frac{\hat{\alpha}}{2}\right) \\ &+ 2\sqrt{x\Gamma_L\Gamma_R} \left[ \left(1 + \frac{\hat{\alpha}}{2}\right) M^\dagger \hat{g}_{RL} \left(1 + \frac{\hat{\alpha}}{2}\right) \right. \\ &\left. + \left(1 - \frac{\hat{\alpha}}{2}\right) \hat{g}_{LR} M \left(1 - \frac{\hat{\alpha}}{2}\right) \right]. \end{aligned} \quad (16)$$

The matrix  $M$  is  $M = e^{i\phi\tau_z} U = I\nu + i\vec{n}\vec{\tau}$  where  $\nu = \cos\theta \cos\phi$ ,  $\vec{n} = (\sin\phi \sin\theta/2, \cos\phi \sin\theta/2, \sin\phi \cos\theta/2)$  and  $\tau_i$  are Pauli matrices in spin space. Here we introduce the tunneling widths:  $\Gamma_{L,R} = 2\pi N_{L,R} t^2$ . Taking  $\alpha = 0$  and inverting  $G^{-1}$  we find the GFs of the dot interacting with the leads (see Appendix A). As we find below, the resonance contribution to the noise is related to terms that involve the matrices  $M, M^\dagger$  [or  $C(\epsilon, \epsilon')$  in Eq. (C6)]. We find that the result for the resonance term does not depend on which combination of currents  $J_{L \rightarrow d}$  and  $J_{d \rightarrow R}$  [determining the source terms  $\alpha$  in Eq. (16)] are used. We checked this statement by using different definitions for the total current, i.e., taking  $\alpha = 0$  in various terms of Eq. (16).

Integrating out the dot fermions  $d$  with the action (15) we arrive at the generating functional  $Z_{\text{dot}}(\alpha) = \det G^{-1} = \exp[\text{Tr} \ln G^{-1}]$  which depends on the vertex function  $Q(\alpha)$ . Similar to Eq. (13) the current through the dot is

$$J_d(t) = \frac{\delta \ln Z_d}{\delta \alpha(t)} = -\text{Tr} \left[ G \frac{\delta Q(\alpha)}{\delta \alpha(t)} \right]. \quad (17)$$

Performing calculations for the case of equal tunneling widths  $\Gamma_L = \Gamma_R$  (see Appendix B) we obtain the current:  $J_{\text{dot}} =$

$e(J_{d1} + J_{d2} + J_{d3})$  where

$$J_{d1} = \bar{\Gamma}(1 - 2T_B) \sum_{\sigma} \int \frac{d\epsilon}{2\pi} \text{Im} G_{\sigma}^R(\epsilon) \Delta_{\epsilon}^{(-)} \quad (18)$$

$$J_{d2} = -2\nu \bar{\Gamma} \sqrt{R_B T_B} \sum_{\sigma} \int \frac{d\epsilon}{2\pi} \text{Re} G_{\sigma}^R(\epsilon) \Delta_{\epsilon}^{(-)} \quad (19)$$

$$J_{d3} = T_B \bar{\Gamma}^2 \int \frac{d\epsilon}{2\pi} \text{Tr} [G^R(\epsilon)(\vec{n}\vec{\tau})G^A(\epsilon)(\vec{n}\vec{\tau})] \Delta_{\epsilon}^{(-)}. \quad (20)$$

Here  $\bar{\Gamma} = (\Gamma_L + \Gamma_R)/(2(1+x))$  and  $\Delta_{\epsilon}^{(\mp)} = f_L(\epsilon) \mp f_R(\epsilon)$ . The trace in the last equation (20) is

$$\begin{aligned} \text{Tr}[\dots] &= \sum_{\sigma} \left[ -\frac{\sin^2 \phi \cos^2 \theta/2}{\bar{\Gamma}} \text{Im} G_{\sigma}^R(\epsilon) \right. \\ &\left. + \sin^2(\theta/2) G_{\sigma}^R G_{-\sigma}^A \right], \end{aligned} \quad (21)$$

which presents two different scattering processes. The first term with  $\sin^2 \phi$  appears also for an Aharonov-Bohm phase and for  $\theta = 0$  the corresponding current coincides with that in Ref. 22; this term does not depend on the sign of phase  $\phi$  maintaining the relation  $G(\phi) = G(-\phi)$  for conductance in closed system (two-terminal setup).

We note that for  $\theta = 0$  the two spin states decouple and a resonance phenomena at the Larmor frequency is not possible. There are still interference effects due to the phase  $\phi$ , though these are unrelated to the resonance. The second term of Eq. (21) describes the spin orbit effect and reflects tunneling transitions accompanied by spin flips. The phase  $\theta$  is therefore controlling the ESR effect.

### IV. CURRENT SPECTRAL DENSITY

The current noise power  $S_d$  is given by formula (14) in which  $Z_W$  is replaced by  $Z_{\text{dot}}$ . The total noise function can be written as a sum of two terms  $S_d(t, t') = S_{d1}(t, t') + S_{d2}(t, t')$

$$S_{d1}(t, t') = -\text{Tr} \left[ G \frac{\delta^2 Q}{\delta \alpha(t) \delta \alpha(t')} \right] \quad (22)$$

$$S_{d2}(t, t') = -\text{Tr} \left[ G \frac{\delta Q}{\delta \alpha(t)} G \frac{\delta Q}{\delta \alpha(t')} \right]. \quad (23)$$

We calculate the current spectral density to lowest order in  $W$  for these terms that contain a resonance contribution at Larmor frequency. Details of the derivation are given in Appendix C. We write the frequency dependent noise  $S_{d1}(\omega)$  and  $S_{d2}(\omega)$  as an expansion in  $W \sim \sqrt{x}$ :

$$\begin{aligned} S_{d1}(\omega) &= S^0(\omega) + \sqrt{x} S^1(\omega) + x S^2(\omega) \\ S_{d2}(\omega) &= S_0(\omega) + \sqrt{x} S_1(\omega) + x S_2(\omega). \end{aligned} \quad (24)$$

The spin flip transport which is responsible for the resonance occurs due to the spin-orbit interacting vertices. This effect takes place at least in the terms linear in  $x$  ( $S^2, S_2$ ) which are presented below (all other contributions to the noise power are given explicitly in Appendix C). The first term depends weakly on frequency

$$\begin{aligned} S^2(\omega) &= \frac{3e^2 \bar{\Gamma}^2}{4(1+x)^2} \int \frac{d\epsilon}{2\pi} \text{Tr} (G^R(\epsilon) \vec{n}\vec{\tau} G^A(\epsilon) \vec{n}\vec{\tau}) \\ &\times [\Delta_{\epsilon-\omega}^{(-)} + \Delta_{\epsilon+\omega}^{(-)}] \Delta_{\epsilon}^{(-)}. \end{aligned} \quad (25)$$

The second term  $S_2$  contains three contributions

$$S_2(\omega) = S_2^{RR+AA} + S_2^{RA} + S_2^K, \quad (26)$$

where

$$\begin{aligned} S_2^{RR+AA} &= \frac{e^2 \bar{\Gamma}^2}{4(1+x)^2} \int \frac{d\epsilon}{2\pi} (\hat{n}^{RR} + \hat{n}^{AA}) \Delta_{\epsilon-\omega/2}^{(+)} \Delta_{\epsilon+\omega/2}^{(+)} \\ S_2^{RA} &= e^2 \bar{\Gamma}^2 \int \frac{d\epsilon}{2\pi} (\hat{n}^{RA} + \hat{n}^{AR}) \\ &\quad \times \left[ 1 - \frac{f_L(\epsilon - \omega/2) f_R(\epsilon + \omega/2) + (\omega \rightarrow -\omega)}{1+x} \right] \\ S_2^K &= e^2 \bar{\Gamma}^2 \sqrt{R_B} \int \frac{d\epsilon}{2\pi} \text{Tr} \{ \hat{m} \Delta_{\epsilon-\omega/2}^{(+)} \Delta_{\epsilon+\omega/2}^{(+)} \\ &\quad + \frac{\bar{\Gamma}}{1+x} [\text{Im} G^R(\epsilon - \omega/2) \bar{n} \bar{\tau} G^R(\epsilon + \omega/2) \bar{n} \bar{\tau} \\ &\quad \times G^A(\epsilon + \omega/2) \Delta_{\epsilon-\omega/2}^{(-)} \Delta_{\epsilon+\omega/2}^{(-)} + (\omega \rightarrow -\omega)] \} \end{aligned}$$

here

$$\begin{aligned} \hat{n}^{MN} &= \text{Tr} [G^M(\epsilon - \omega/2) \bar{n} \bar{\tau} G^N(\epsilon + \omega/2) \bar{n} \bar{\tau}] \\ \hat{m} &= \text{Im} G^R(\epsilon - \omega/2) \bar{n} \bar{\tau} \text{Im} G^R(\epsilon + \omega/2) \bar{n} \bar{\tau}, \end{aligned}$$

where  $M, N = R(A)$ .

The resonance behavior at  $\omega = 2H$  that we find is related to  $S_2(\omega)$ . We note first, as is easy to check, that the total noise power (at  $\omega \rightarrow 0$ )  $S_d \rightarrow 0$  in each order in  $W$  if  $T > V$  and  $T \rightarrow 0$ . This observation serves as additional test for our calculations.

Separating the resonance contributions in the expression for  $S_2(\omega)$  yields at the principal result of our work:  $S_2^{\text{sing}} = S_2^r + S_2^s$  where

$$\begin{aligned} S_2^r &= 2e^2 \bar{\Gamma}^2 \sin^2 \theta / 2 \sum_{\sigma} \int \frac{d\epsilon}{2\pi} \text{Im} G_{\sigma}^R(\epsilon - \omega/2) \\ &\quad \times \text{Im} G_{-\sigma}^R(\epsilon + \omega/2) F(\epsilon, \omega); \quad (27) \end{aligned}$$

$$\begin{aligned} F(\epsilon, \omega) &= 1 - \frac{1}{4} [3(f_L(\epsilon - \omega/2) f_R(\epsilon + \omega/2) + (\omega \rightarrow -\omega)) \\ &\quad - (f_R(\epsilon - \omega/2) f_R(\epsilon + \omega/2) + (R \rightarrow L))] \quad (28) \end{aligned}$$

$$\begin{aligned} S_2^s &= e^2 \bar{\Gamma}^3 \sin^2 \theta / 2 \sum_{\sigma} \int \frac{d\epsilon}{2\pi} [\text{Im} G_{\sigma}^R(\epsilon - \omega/2) \\ &\quad \times \text{Im} G_{-\sigma}^R(\epsilon + \omega/2) \text{Im} G_{\sigma}^R(\epsilon + \omega/2) \\ &\quad \times \Delta_{\epsilon-\omega/2}^{(-)} \Delta_{\epsilon+\omega/2}^{(-)} + (\omega \rightarrow -\omega)] \quad (29) \end{aligned}$$

There is a potentially singular contribution that also in  $S^{(2)}$

$$\begin{aligned} S^{(2)\text{sing}} &= \frac{3e^2 \bar{\Gamma}^2}{4} \sin^2 \theta / 2 \sum_{\sigma} \int \frac{d\epsilon}{2\pi} \text{Im} G_{\sigma}^R(\epsilon) \text{Im} G_{-\sigma}^R(\epsilon) \\ &\quad \times [\Delta_{\epsilon-\omega}^{(-)} + \Delta_{\epsilon+\omega}^{(-)}] \Delta_{\epsilon}^{(-)}. \quad (30) \end{aligned}$$

However, it can be seen that this term depends weakly on frequency and therefore it does not have a resonance at the Larmor frequency.

In the experiments<sup>1</sup> the parameters satisfy  $V \gg T \gg 2H$ . Therefore, if the mean level position  $\epsilon_0$  is in between the two chemical potentials  $-\frac{1}{2}V < \epsilon_0 < \frac{1}{2}V$  and is not too close to  $\pm \frac{1}{2}V$ , i.e.,  $|\epsilon_0 \pm \frac{1}{2}V| \gtrsim H$ , then we have  $F(\epsilon, \omega) \simeq 3$  and

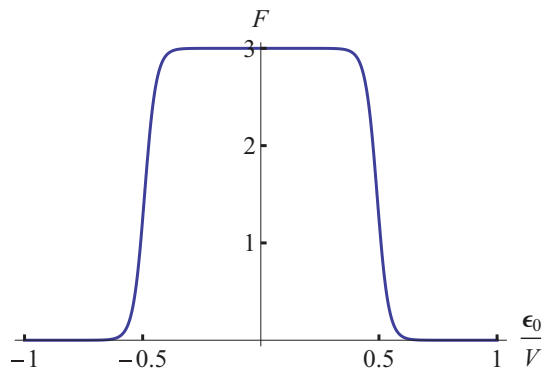


FIG. 1. (Color online) Dependence of the noise on the mean level position  $\epsilon_0$ , the function  $F(\epsilon_0)$  in Eq. (28) neglecting  $\omega, H$  terms (i.e., valid for  $|\epsilon_0 \pm \frac{1}{2}V| \gtrsim H$ ). The voltage and temperature ratio is  $\frac{V}{T} = 40$ .

$\Delta_{\epsilon \pm \omega/2} \simeq 2$ . We show in particular the function  $F(\epsilon_0)$  of Eq. (28), neglecting  $\omega$  and  $H$  terms, in Fig. 1.

Taking  $F(\epsilon, \omega) \simeq 3$  and  $\Delta_{\epsilon \pm \omega/2}^- \simeq 2$  and using Eq. (A12) the integrals are simply evaluated:

$$\begin{aligned} S_2^r &\simeq \frac{3\pi e^2 \sin^2 \frac{1}{2}\theta}{2\pi} \sum_{\sigma} \frac{\bar{\Gamma}^3}{(\omega/2 + \sigma H)^2 + \bar{\Gamma}^2} \quad (31) \\ S_2^s &\simeq \frac{\pi e^2 \bar{\Gamma}^5 \sin^2 \frac{1}{2}\theta}{2\pi(H^2 + \bar{\Gamma}^2)} \sum_{\sigma} \frac{[(\frac{1}{2}\omega + \sigma H)^2 + 3\bar{\Gamma}^2 - \frac{1}{2}\sigma\omega H]}{[(\frac{1}{2}\omega + \sigma H)^2 + \bar{\Gamma}^2](\bar{\Gamma}^2 + \omega^2)}. \quad (32) \end{aligned}$$

In standard units the  $2\pi$  in the denominators are replaced by  $h$ . Thus the last equations (31) and (32) show the resonance behavior of the noise power at  $\omega = \pm 2H$ .

In Fig. 2 we plot the noise power  $S_3(\omega) = S_2^r + S_2^s$ , Eqs. (31) and (32), normalized by  $S_b = \frac{\pi}{2h} e^2 H \sin^2 \frac{1}{2}\theta$  as a function of frequency. For a sharp resonance, as seen experimentally<sup>1</sup>  $\bar{\Gamma} \ll 2H$  since  $\bar{\Gamma}$  determines the resonance width. Therefore the ratio  $S_2^s/S_2^r \approx \bar{\Gamma}^2/H^2 \ll 1$  is small and  $S_2^r$  with the Lorentzian shape dominates. In the wide range where  $F = 3$  (Fig. 1) we

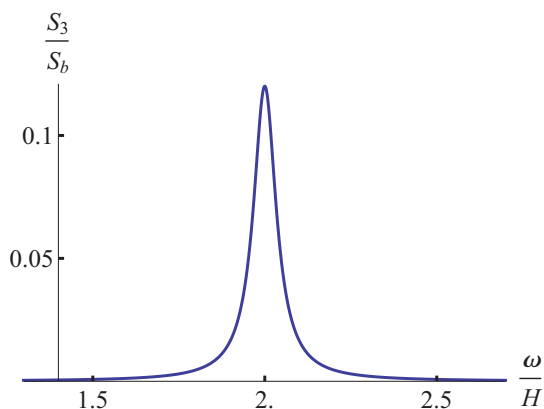


FIG. 2. (Color online) The current spectral power  $S_3(\omega)$  which is a sum of two resonance contributions (31) and (32) showing resonance peaks at  $\omega = \pm 2H$ . The width parameter is  $\bar{\Gamma}/H = 0.02$ .



have therefore for the signal amplitude at resonance

$$S_{\text{signal}} = \frac{e^2}{h} 3\pi \bar{\Gamma} x \sin^2 \frac{1}{2}\theta. \quad (33)$$

We note also that at  $x \gg 1$  where  $\bar{\Gamma}x \rightarrow \Gamma$  another term causes a cancellation of this one (Appendix C) and the signal vanishes at large  $x$ . We expect then that the signal is maximal at  $x \approx 1$ , in accordance with numerical data.<sup>19</sup>

## V. CONCLUSION

We have considered a general spin-orbit scattering mechanism in a setup of a nanoscopic interferometer and have shown that the interference of the two transmission paths leads to a resonance contribution to the current correlation spectral density at the Larmor frequency. In particular we find that the effect takes place in the absence of lead polarizations, consistent with ESR-STM experiments. Our model also accounts for several unusual features of the data: (i) A sharp resonance even at high temperatures  $T \gg H$ , (ii) insensitivity to the details of the spin defect, i.e., to the positions of its levels between the tip and substrate chemical potentials, (iii) contour plots<sup>2,3</sup> showing that the signal is maximal at  $\sim 1$  nm from a center, hence a significant direct coupling  $W$  bypassing the spin can be achieved.

Here we have neglected the Coulomb interaction  $U$  between charges on the dot. However, for the experimentally interesting case of a large applied voltage  $V$ , the Coulomb repulsion is expected to satisfy  $U \lesssim eV$ . The levels therefore remain between the two chemical potentials and we expect that the resonance part of the noise is weakly affected by  $U$ . A similar conclusion was reached for the case with polarized leads.<sup>13</sup>

The limit  $U \rightarrow \infty$  for a temperature or voltage higher than the Kondo temperature can be estimated by replacing the dot GF by<sup>29</sup>  $G_{0,\sigma}^R(\epsilon) \rightarrow (1 - \langle n_{-\sigma} \rangle) G_{0,\sigma}^R(\epsilon)$  where the average occupancy  $\langle n_{\sigma} \rangle$  is determined self-consistently by multiplying the right hand side of Eq. (A16) by  $(1 - \langle n_{-\sigma} \rangle)$ , hence  $\langle n_{\sigma} \rangle = -\frac{1}{2}(1 - \langle n_{-\sigma} \rangle)[\frac{1}{2}f_L(\epsilon_0) + \frac{1}{2}f_R(\epsilon_0) - 1]$ . We find that for equal occupancies of the two spin states  $\langle n_{\sigma} \rangle$  interpolates between  $\frac{1}{2}$  at  $\epsilon_0 \ll \frac{1}{2}V$  to zero at  $\epsilon_0 \gg \frac{1}{2}V$ , as expected. In the important range of  $|\epsilon_0| < \frac{1}{2}V - T$  (see Fig. 1) we obtain  $\langle n_{\sigma} \rangle = \frac{\Gamma_R}{2\Gamma_R + \Gamma_L}$ , i.e.,  $\langle n_{\sigma} \rangle = \frac{1}{3}$  in the symmetric case. With this estimate, the resonance term involving a product of two dot GFs has a factor  $(\frac{\Gamma_R + \Gamma_L}{2\Gamma_R + \Gamma_L})^2$ . We expect therefore that Coulomb interactions on the dot reduce the resonance term by up to a factor between 1 and  $\frac{1}{4}$ , e.g.,  $\frac{4}{9}$  in the symmetric case.

We proceed to estimate the spin-orbit coupling. We consider first doped Si, the substrate with which most of the ESR-STM data were taken. A Rashba spin-orbit coupling was measured<sup>30</sup> as  $\bar{\alpha} = 0.55 \cdot 10^{-12}$  eV cm. This coupling is proportional to the external electric field that is estimated<sup>31</sup> as  $3 \times 10^6$  V/m. In the STM experiment the tip voltage of 1–2 V at a distance of  $\sim 1$  nm from the substrate produces a field of  $\approx 10^9$  V/m. Therefore the spin-orbit coupling is enhanced to  $\bar{\alpha} \sim 10^{-9}$  eV cm. We consider next the STM Tungsten (W) tip, that turns out to have a stronger  $\bar{\alpha}$ . Data<sup>32</sup> on clean W(110) and on one monolayer H on W(110) show a spin-orbit splitting of 0.5 eV at wave vector

$k \approx 0.3 \text{ \AA}^{-1}$ . Further data<sup>33</sup> on W(110) shows a spin-orbit splitting of  $\sim 0.2$  eV, increasing to 0.5 eV at 0.5 monolayers of Li, reflecting an enhancement of the W spin orbit by the electric field induced by the Li coverage.<sup>33</sup> We infer that  $\bar{\alpha} \approx 10^{-8}$  eV cm on the Tungsten tip, a value that is likely to be enhanced by the strong tip-substrate electric field.

We next estimate the spin-flip angle  $\theta$  by extending Bardeen's formula<sup>34,35</sup> for the spin-diagonal tunneling  $t \sin \frac{1}{2}\theta$  to include spin-orbit coupling. The spin-orbit term reduces to a similar surface overlap, except for the absence of a gradient term. The ratio of the two couplings is then  $\tan \frac{1}{2}\theta = \frac{2m}{\hbar^2} \bar{\alpha} \xi$  where  $m$  is the electron mass and  $\xi$  is the scale for wavefunction variation parallel to the substrate,<sup>35</sup> i.e., of the order of the tip size  $\sim 1$  nm. Hence  $\tan \frac{1}{2}\theta \approx 1$ , and possibly larger due to the tip-substrate electric field. We expect that lowering the voltage, or replacing the tip by a metal with weaker spin-orbit coupling will reduce the resonance intensity.

Our key result Eq. (33) shows that the signal amplitude is  $S_{\text{signal}} \sim t^2 W^2$ . The signal should vanish at  $W = 0$  on general grounds,<sup>19</sup> yet the  $W^2$  form is unexpected. Some of our other results can be obtained for small  $t, W$  by simple estimates: The resonance linewidth follows from a golden rule  $\Gamma = 2\pi t^2 N(0)$ ; the DC current via the dot  $J_d = 2e\Gamma/\hbar$  for  $eV \gg 2H, T$  [Eq. (18) is the dominant term] corresponds to a transition rate  $\Gamma/\hbar$  from either reservoir to the dot, hence  $J_d = 2e\Gamma/\hbar$  given the dot's two states. The direct transport of  $L \rightarrow R$  is also a golden rule  $\Gamma_W = 2\pi W^2 N_L(0)$  times the final number of states  $N_R(0)$  eV, hence  $J_W = \frac{2e^2}{h} 4xV$  (for  $x \ll 1$ ) while the corresponding background noise is a classical shot noise  $S_W = 2eJ_W$ , Eq. (A9). The noise of the dot current is, however, much reduced from that of a shot noise since  $S^0 \approx \frac{1}{4}eJ_d$ , Eq. (C4).

To analyze the experimental data we first estimate the relevant parameters. The resonance linewidth is  $\sim 1$  MHz =  $\Gamma/2\pi = t^2 N(0)/\hbar$  (for  $x \ll 1$ ). Assuming a metallic  $N(0) \sim 1/(5 \text{ eV})$  yields  $tN(0) \approx 10^{-5}$ . Considering next the DC current 0.1–1 nA at  $\sim 1$  V: The dot current for  $x \ll 1$   $J_d = 2e\Gamma/\hbar \approx 10^{-12}$  A is too small, hence the DC current is dominated by the direct coupling  $W$  with  $J_W = \frac{2e^2}{h} 4xV$ , hence  $WN(0) \approx 10^{-3}$  and  $W \gg t$ . The background noise due to the dot current is  $S_0 \approx e^2\Gamma/\hbar$  while that from  $W$  is  $S_W = \frac{2e^2}{h} 8x \text{ eV}$ , hence  $\frac{S_0}{S_W} \approx \frac{t^2}{W^2}/[8N(0) \text{ eV}] \ll 1$ , i.e., the background noise is dominated by  $S_W$ .

We note that the background noise is not measured in the experiment since the modulation technique<sup>1</sup> measures the derivative of the noise spectra. Furthermore, the signal intensity is under study<sup>36</sup> as is highly sensitive to uncertainties in the feedback and impedance matching circuits. We find that the signal to background intensity for  $x \ll 1$  is  $S_{\text{signal}}/S_W = \frac{3\pi}{16} \sin^2 \frac{1}{2}\theta \frac{\Gamma}{eV}$ , i.e., of the order of  $10^{-9}$ – $10^{-8}$ . In conclusion, our model presents an analytic solution to a long standing puzzle, paving the way for more controlled single spin detection via ESR-STM.

## ACKNOWLEDGMENTS

We are thankful for stimulating discussions with Y. Manassen, C. Berthod, O. Entin-Wohlman, S. A. Gurvitz, A. Janossy, L. S. Levitov, I. Martin, Y. Meir, M. Y. Simmons,

F. Simon, E. I. Rashba, S. Rogge, A. Shnirman, G. Zárnd, and A. Yazdani. This research was supported by The Israel Science Foundation (BIKURA) (Grant No. 1302/11) and by the Israel-Taiwanese Scientific Research Cooperation of the Israeli Ministry of Science and Technology.

### APPENDIX A: DIRECT CURRENT AND NOISE. GREEN'S FUNCTIONS

The GFs integrated over momentum are obtained by inverting the inverse Green function in Eq. (9), as shown for the diagonal terms in Eq. (11). Here we write the whole list of these functions:

$$\begin{aligned}\bar{g}_{LL} &= 2\pi N_L D_L^{-1} \bar{g}_L = 2\pi N_L \hat{g}_{LL} \\ \bar{g}_{RR} &= 2\pi N_R D_R^{-1} \bar{g}_R = 2\pi N_R \hat{g}_{RR} \\ \bar{g}_{RL} &= 2\pi N_R W \bar{g}_R (1 - \hat{\alpha}) e^{-\phi\sigma} \bar{g}_{LL} \\ &= (2\pi)^2 N_R N_L W e^{-\phi\sigma} \hat{g}_{RL} \\ \bar{g}_{LR} &= 2\pi N_R W \bar{g}_{LL} (1 + \hat{\alpha}) e^{\phi\sigma} \bar{g}_R \\ &= (2\pi)^2 N_R N_L W \hat{g}_{LR} e^{\phi\sigma}.\end{aligned}\quad (\text{A1})$$

Explicitly for  $\alpha = 0$  we can write

$$\bar{g}_{LL}^{R,A}(\epsilon) = 2\pi N_L \frac{\mp i}{2(1+x)} \quad (\text{A2})$$

$$\bar{g}_{LL}^K(\epsilon) = \frac{-2\pi N_L i}{(1+x)^2} (f_L(\epsilon) + x f_R(\epsilon)). \quad (\text{A3})$$

Changing R to L yields  $\bar{g}_{RR}$ . The off-diagonal functions acquire a form

$$\hat{g}_{RL}^{R,A} = -\frac{1}{4(1+x)}, \quad \hat{g}_{RL}^K = \frac{-1}{2(1+x)^2} \Delta_\epsilon^{(-)} \quad (\text{A4})$$

$$\hat{g}_{LR}^{R,A} = -\frac{1}{4(1+x)}, \quad \hat{g}_{LR}^K = \frac{1}{2(1+x)^2} \Delta_\epsilon^{(-)} \quad (\text{A5})$$

$$\Delta_\epsilon^{(\pm)} = \tanh \frac{\epsilon + V/2}{2T} \pm \tanh \frac{\epsilon - V/2}{2T}. \quad (\text{A6})$$

With the help of these functions we find the direct tunneling current and the corresponding noise power which acquire standard forms (below  $\sigma_i$  are Pauli matrices that act in Keldysh space)

$$J_W(t) = \text{Tr} \left[ g_{LR} \frac{\delta g_{LR}^{-1}}{\delta \alpha(t)} + g_{RL} \frac{\delta g_{RL}^{-1}}{\delta \alpha(t)} \right] \quad (\text{A7})$$

$$J_W = 2eT_B \int \frac{d\epsilon}{2\pi} \Delta_\epsilon^{(-)} \quad (\text{A8})$$

and

$$\begin{aligned}S_W &= \text{Tr} \left[ \left( \frac{\delta g_{LR}(\bar{t}t')}{\delta \alpha(t)} - \frac{\delta g_{RL}(\bar{t}t')}{\delta \alpha(t)} \right) \sigma_x \right] \\ S_W(0) &= \frac{4e^2}{2\pi} \left[ eV T_B (1 - T_B) \coth \frac{V}{2T} + 2T_B^2 T \right]. \quad (\text{A9})\end{aligned}$$

The noise  $S_W(\omega)$  is well known<sup>28</sup> and coincides with Eq. (A9) for small  $\omega$ ,  $\omega \ll eV$ . The effective action of the dot is given by Eq. (15). In the limit of vanishing source terms the corresponding GFs are obtained by inverting  $G^{-1}$  ( $\alpha = 0$ )

$$G_\sigma^R(\epsilon) = \frac{1}{\epsilon - \epsilon_\sigma + r + \frac{i(\Gamma_L + \Gamma_R)}{2(1+x)}} \quad (\text{A10})$$

$$r = \frac{\nu \sqrt{x\Gamma_L\Gamma_R}}{1+x}$$

$$G_\sigma^R(\epsilon) G_\sigma^A(\epsilon) = -\frac{2(1+x)}{\Gamma_L + \Gamma_R} \text{Im} G_\sigma^R(\epsilon) \quad (\text{A11})$$

$$\text{Im} G_\sigma^R(\epsilon) = \frac{-\bar{\Gamma}}{(\epsilon - \epsilon_\sigma + r)^2 + \bar{\Gamma}^2}, \quad (\text{A12})$$

$$\begin{aligned}G^K(\epsilon) &= \frac{2i \text{Im} G^R(\epsilon)}{(1+x)(\Gamma_L + \Gamma_R)} \\ &\times [f_L(\epsilon)(\Gamma_L + x\Gamma_R) + f_R(\epsilon)(x\Gamma_L + \Gamma_R)] \\ &+ 2i \frac{\sqrt{x\Gamma_L\Gamma_R}}{(1+x)^2} \Delta_\epsilon^{(-)} G^R(\epsilon) \bar{n} \bar{\tau} G^A(\epsilon).\end{aligned}\quad (\text{A13})$$

We note also the relation

$$-i G_\sigma^{12}(\epsilon) = -\frac{1}{2} i [G_\sigma^K(\epsilon) - 2i \text{Im} G_\sigma^R(\epsilon)]. \quad (\text{A14})$$

For the effect of Coulomb interactions, as discussed in the conclusions, we need the average occupation on the dot for  $x = 0$ ,

$$\langle n_\sigma \rangle = \int \frac{d\epsilon}{2\pi} \text{Im} G_\sigma^R(\epsilon) \left[ \frac{\Gamma_L f_L(\epsilon) + \Gamma_R f_R(\epsilon)}{\Gamma_L + \Gamma_R} - 1 \right]. \quad (\text{A15})$$

For small widths  $\Gamma_L, \Gamma_R \ll T$  and assuming  $H \ll T$  this yields

$$\langle n_\sigma \rangle = -\frac{1}{2} \left[ \frac{\Gamma_L f_L(\epsilon_0) + \Gamma_R f_R(\epsilon_0)}{\Gamma_L + \Gamma_R} - 1 \right], \quad (\text{A16})$$

which shows that  $\langle n_\sigma \rangle$  interpolates between 1 at  $\epsilon_0 \ll -\frac{1}{2}V$  to zero at  $\epsilon_0 \gg \frac{1}{2}V$ . In the important range of  $|\epsilon_0| < \frac{1}{2}V - T$  (see Fig. 1)  $\langle n_\sigma \rangle = \frac{\Gamma_R}{\Gamma_L + \Gamma_R}$ , i.e.,  $\langle n_\sigma \rangle = \frac{1}{2}$  in the symmetric case.

**APPENDIX B: CURRENT THROUGH THE DOT**

Next we calculate the transmission through the dot which is presented by Eq. (17). The superscripts in the following correspond to matrix elements in Keldysh space,

$$\begin{aligned}
 J_d(t) &= \text{Tr} \left[ G^R \left( \frac{\delta Q(\alpha)}{\delta \alpha(t)} \right)^{11} + G^K \left( \frac{\delta Q(\alpha)}{\delta \alpha(t)} \right)^{21} + G^A \left( \frac{\delta Q(\alpha)}{\delta \alpha(t)} \right)^{22} \right] \\
 \frac{\delta Q(\alpha)}{\delta \alpha(t)} &= \frac{1}{4} \left[ -\Gamma_L \left( \sigma_x \hat{g}_{LL}(t\bar{t}) \left( 1 + \frac{\hat{\alpha}}{2} \right) - \left( 1 - \frac{\hat{\alpha}}{2} \right) \hat{g}_{LL}(\bar{t}t) \sigma_x \right) + \Gamma_R \left( \sigma_x \hat{g}_{RR}(t\bar{t}) \left( 1 - \frac{\hat{\alpha}}{2} \right) - \left( 1 + \frac{\hat{\alpha}}{2} \right) \hat{g}_{RR}(\bar{t}t) \sigma_x \right) \right. \\
 &\quad + 2\sqrt{x\Gamma_L\Gamma_R} \left( \sigma_x M^\dagger \hat{g}_{RL} \left( 1 + \frac{\hat{\alpha}}{2} \right) + \left( 1 + \frac{\hat{\alpha}}{2} \right) M^\dagger \hat{g}_{RL} \sigma_x - \sigma_x \hat{g}_{LR} M \left( 1 - \frac{\hat{\alpha}}{2} \right) - \left( 1 - \frac{\hat{\alpha}}{2} \right) \hat{g}_{LR} M \sigma_x \right) \\
 &\quad \left. + \Gamma_L \frac{\delta \hat{g}_{LL}(t_1 t_2)}{\delta \alpha(t)} + \Gamma_R \frac{\delta \hat{g}_{RR}(t_1 t_2)}{\delta \alpha(t)} + 2\sqrt{x\Gamma_L\Gamma_R} \left[ \frac{\delta \hat{g}_{LR}(t_1 t_2)}{\delta \alpha(t)} M + M^\dagger \frac{\delta \hat{g}_{RL}(t_1 t_2)}{\delta \alpha(t)} \right] \right]. \tag{B1}
 \end{aligned}$$

The current takes the form

$$\begin{aligned}
 J_d &= e \int \frac{d\epsilon}{2\pi} \text{Tr} \left\{ G(\epsilon) \left\{ \frac{1}{2} \left[ -\Gamma_L (\sigma_x \hat{g}_{LL}(\epsilon) - \hat{g}_{LL}(\epsilon) \sigma_x) + \Gamma_R (\sigma_x \hat{g}_{RR}(\epsilon) - \hat{g}_{RR}(\epsilon) \sigma_x) + 2\sqrt{x\Gamma_L\Gamma_R} (\sigma_x M^\dagger \hat{g}_{RL}(\epsilon) \right. \right. \right. \\
 &\quad \left. \left. + M^\dagger \hat{g}_{RL}(\epsilon) \sigma_x - \sigma_x \hat{g}_{LR}(\epsilon) M - \hat{g}_{LR}(\epsilon) M \sigma_x \right) + \Gamma_L \delta \hat{g}_{LL}(\epsilon, \omega) + \Gamma_R \delta \hat{g}_{RR}(\epsilon, \omega) \right. \right. \\
 &\quad \left. \left. + 2\sqrt{x\Gamma_L\Gamma_R} (\delta \hat{g}_{LR}(\epsilon, \omega) M + M^\dagger \delta \hat{g}_{RL}(\epsilon, \omega)) \right\} \right\}. \tag{B2}
 \end{aligned}$$

The variations of the GFs are given as a Fourier transform,

$$\begin{aligned}
 \delta \hat{g}_{LL}(\epsilon, \omega) &= 4x \hat{g}_{LL}(\epsilon - \omega) [\sigma_x \bar{g}_R(\epsilon) - \bar{g}_R(\epsilon - \omega) \sigma_x] \hat{g}_{LL}(\epsilon) \\
 \delta \hat{g}_{RR}(\epsilon, \omega) &= -4x \hat{g}_{RR}(\epsilon - \omega) [\sigma_x \bar{g}_L(\epsilon) - \bar{g}_L(\epsilon - \omega) \sigma_x] \hat{g}_{RR}(\epsilon) \\
 \delta \hat{g}_{LR}(\epsilon, \omega) &= \hat{g}_{LL}(\epsilon - \omega) \sigma_x \bar{g}_R(\epsilon) + \delta g_{LL}(\epsilon, \omega) (1 + \hat{\alpha}) \bar{g}_R(\epsilon) \\
 \delta \hat{g}_{RL}(\epsilon, \omega) &= -\bar{g}_R(\epsilon - \omega) \sigma_x \hat{g}_{LL}(\epsilon) + \bar{g}_R(\epsilon - \omega) (1 - \hat{\alpha}) \delta g_{LL}(\epsilon, \omega). \tag{B3}
 \end{aligned}$$

Performing the trace in Keldysh space and using the explicit form of the lead GFs Eqs. (A2)–(A5) as well the dot GFs Eqs. (A10)–(A13) we arrive at Eqs. (18)–(20).

**APPENDIX C: CURRENT NOISE POWER**

We consider the current noise power for equal tunneling widths  $\Gamma_L = \Gamma_R$  to order  $x$ . At first we present the derivation of  $S_{d1}$ . This part of the noise power depends on the second variation of the vertex function  $\delta^2 Q$ . Their Fourier transformed Keldysh components acquire a form

$$\begin{aligned}
 (\delta^2 Q)_\omega^{11} &= -\frac{\bar{\Gamma}}{4} \left[ i + 4\sqrt{x\nu} F_{1\omega} + \frac{i\sqrt{x\bar{n}\bar{\nu}}}{1+x} F_{2\omega} - \frac{2ix}{1+x} (4 - F_3 + F_4) \right] \\
 (\delta^2 Q)_\omega^{22} &= \frac{\bar{\Gamma}}{4} \left[ i - 4\sqrt{x\nu} F_{1\omega} + \frac{i\sqrt{x\bar{n}\bar{\nu}}}{1+x} F_{2\omega} - \frac{2ix}{1+x} (4 - F_3 + F_4) \right] \\
 (\delta^2 Q)_\omega^{21} &= \frac{i\bar{\Gamma}}{16} \left[ (\Delta_{\epsilon-\omega}^{(+)} + \Delta_{\epsilon+\omega}^{(+)}) + 6 \frac{\sqrt{x\bar{n}\bar{\nu}}}{1+x} (\Delta_{\epsilon-\omega}^{(-)} + \Delta_{\epsilon+\omega}^{(-)}) \right], \tag{C1}
 \end{aligned}$$

where

$$\begin{aligned}
 F_{1\omega} &= 1 - \frac{(\Delta_L + x\Delta_R) f_R(\epsilon) + \Delta_R (f_L(\epsilon) + x f_R(\epsilon))}{4(1+x)} \\
 F_{2\omega} &= \Delta_L f_R(\epsilon) - \Delta_R f_L(\epsilon) \\
 F_3 &= \frac{1}{1+x} \{ [(f_L(\epsilon) + x f_R(\epsilon)) f_R(\epsilon - \omega) + (L \Leftrightarrow R)] + (\omega \rightarrow -\omega) \} \\
 F_4 &= \sqrt{R_B} \Delta_\epsilon^{(-)} (\Delta_{\epsilon+\omega}^{(-)} + \Delta_{\epsilon-\omega}^{(-)}). \tag{C2}
 \end{aligned}$$

Here  $\Delta_{L,R} = f_{L,R}(\epsilon - \omega) + f_{L,R}(\epsilon + \omega)$ . After tracing Keldysh space we obtain

$$S_{d1} = -\frac{e^2}{2} \text{Tr} [G^R (\delta^2 Q)^{11} + G^K (\delta^2 Q)^{21} + G^A (\delta^2 Q)^{22}]. \tag{C3}$$

Using the explicit forms for vertices (C1) [see also first Eq. (24)] we arrive at

$$S^0(\omega) = -e^2 \frac{\bar{\Gamma}}{2} \int \frac{d\epsilon}{2\pi} \text{Tr} \left\{ \text{Im} G^R(\epsilon) \left[ 1 - \frac{1}{8} (f_L(\epsilon) + f_R(\epsilon)) (\Delta_{\epsilon-\omega}^{(+)} + \Delta_{\epsilon+\omega}^{(+)}) \right] \right\} \quad (\text{C4})$$

$$S^1(\omega) = -e^2 \frac{\bar{\Gamma}}{2} \int \frac{d\epsilon}{2\pi} \text{Tr} \left\{ \text{Im} G^R(\epsilon) \left[ \frac{\bar{n}\bar{\tau}}{1+x} \left( F_{2\omega} - \frac{3}{4} (f_L(\epsilon) + f_R(\epsilon)) (\Delta_{\epsilon-\omega}^{(-)} + \Delta_{\epsilon+\omega}^{(-)}) \right) \right] \right. \\ \left. - 4\nu F_{1\omega} \text{Re} G^R(\epsilon) - \frac{\bar{\Gamma}}{4} G^R(\epsilon) \bar{n}\bar{\tau} G^A(\epsilon) \Delta_{\epsilon}^{(-)} (\Delta_{\epsilon-\omega}^{(+)} + \Delta_{\epsilon+\omega}^{(+)}) \right\} \quad (\text{C5})$$

and the formula for  $S^{(2)}$  is given in the main text Eq. (25).

The other part of the current spectral density  $S_{d2}(\omega)$  [see Eq. (23)] is defined by Fourier transformed GFs and vertices

$$S_{d2}(\omega) = -e^2 \int \frac{d\epsilon}{2\pi} \text{Tr} \left[ G\left(\epsilon - \frac{\omega}{2}\right) \delta Q(\omega) G\left(\epsilon + \frac{\omega}{2}\right) \delta Q(-\omega) \right] \quad (\text{C6}) \\ 2\delta Q(\omega) = A\left(\epsilon + \frac{\omega}{2}\right) + B\left(\epsilon - \frac{\omega}{2}\right) + C\left(\epsilon - \frac{\omega}{2}, \epsilon + \frac{\omega}{2}\right) + 4xD\left(\epsilon - \frac{\omega}{2}, \epsilon + \frac{\omega}{2}\right) + 8x\sqrt{x}E\left(\epsilon - \frac{\omega}{2}, \epsilon + \frac{\omega}{2}\right),$$

where

$$A(\epsilon) = \frac{\Gamma}{2} \sigma_x \{ -(\hat{g}_{LL}(\epsilon) - \hat{g}_{RR}(\epsilon)) + 2\sqrt{x} [M^\dagger g_R(\epsilon) \hat{g}_{LL}(\epsilon) - \hat{g}_{LL}(\epsilon) g_R(\epsilon) M] \} \\ B(\epsilon) = \frac{\Gamma}{2} \{ \hat{g}_{LL}(\epsilon) - \hat{g}_{RR}(\epsilon) + 2\sqrt{x} [M^\dagger g_R(\epsilon) \hat{g}_{LL}(\epsilon) - \hat{g}_{LL}(\epsilon) g_R(\epsilon) M] \} \sigma_x \\ C(\epsilon, \epsilon') = 2\sqrt{x} \Gamma [ \hat{g}_{LL}(\epsilon) \sigma_x g_R(\epsilon') M - M^\dagger g_R(\epsilon) \sigma_x \hat{g}_{LL}(\epsilon') ] \\ D(\epsilon, \epsilon') = \Gamma [ \hat{g}_{LL}(\epsilon) (\sigma_x g_R(\epsilon') - g_R(\epsilon) \sigma_x) \hat{g}_{LL}(\epsilon') ] - (L \Leftrightarrow R) \quad (\text{C7})$$

and

$$E\left(\epsilon - \frac{\omega}{2}, \epsilon + \frac{\omega}{2}\right) = \hat{Y} g_R\left(\epsilon + \frac{\omega}{2}\right) M + M^\dagger g_R\left(\epsilon - \frac{\omega}{2}\right) \hat{Y} \\ \hat{Y} = \Gamma \hat{g}_{LL}\left(\epsilon - \frac{\omega}{2}\right) \left[ \sigma_x g_R\left(\epsilon + \frac{\omega}{2}\right) - g_R\left(\epsilon - \frac{\omega}{2}\right) \sigma_x \right] \hat{g}_{LL}\left(\epsilon + \frac{\omega}{2}\right). \quad (\text{C8})$$

Indeed the vertex function  $D(\epsilon, \epsilon')$  is irrelevant for spin flip processes and may be ignored. Explicit form for Keldysh components of  $\delta Q(\omega)$  to linear order in  $x$  can be simply found:

$$\delta Q^{21}(\omega) = i\bar{\Gamma} \sqrt{x} \bar{n}\bar{\tau} \\ \delta Q^{11}(\omega) = -\frac{\bar{\Gamma} \sqrt{R_B}}{4} i \Delta_{\epsilon-\omega/2}^{(-)} - \frac{\bar{\Gamma} \sqrt{x}}{2(1+x)} \left[ \left( 2\nu \Delta_{\epsilon-\omega/2}^{(-)} + 2i\bar{n}\bar{\tau} (x f_R(\epsilon - \omega/2)) + \frac{1}{2} \Delta_{\epsilon-\omega/2}^{(+)} \right) \right] \\ \delta Q^{22}(\omega) = \frac{\bar{\Gamma} \sqrt{R_B}}{4} i \Delta_{\epsilon+\omega/2}^{(-)} - \frac{\bar{\Gamma} \sqrt{x}}{2(1+x)} \left[ \left( 2\nu \Delta_{\epsilon+\omega/2}^{(-)} - 2i\bar{n}\bar{\tau} (x f_R(\epsilon + \omega/2)) + \frac{1}{2} \Delta_{\epsilon+\omega/2}^{(+)} \right) \right] \\ \delta Q^{12}(\omega) = \frac{\bar{\Gamma} \sqrt{x}}{1+x} \{ i\bar{n}\bar{\tau} [1+x - (f_R(\epsilon + \omega/2)(f_L(\epsilon - \omega/2) + x f_R(\epsilon - \omega/2)) + (\omega \rightarrow -\omega))] \\ - \nu [f_R(\epsilon + \omega/2) f_L(\epsilon - \omega/2) - (\omega \rightarrow -\omega)] \}. \quad (\text{C9})$$

These formulas for  $\delta Q(\omega)$  can be applied for all  $x$  if modifications which come from  $D(\epsilon, \epsilon')$  and  $E(\epsilon, \epsilon')$  vertices are included.  $D(\epsilon, \epsilon')$  introduces a factor  $1 + T_B(3-x)/2\sqrt{R_B}$  into the first term in expressions for  $\delta Q^{11}(\omega)$  and  $\delta Q^{22}(\omega)$ . There is also a contribution to  $\delta Q^{12}(\omega)$ :  $i T_B \bar{\Gamma} (f_L(\epsilon + \omega/2) f_L(\epsilon - \omega/2) - (L \rightarrow R))$ . All these additions do not influence the resonance part of the tunneling. If we consider the limit of large  $x$  the vertex  $E(\epsilon, \epsilon')$  is important. In this case we obtain that an apparent constant term in Eq. (33) cancels in the vertex  $\delta Q(\omega)$ , hence the resonance term vanishes at large  $x$ .

With the help of these vertex functions we calculate all parts of the  $S_{d2}$  noise power [see Eq. (24)]:

$$S_0(\omega) = \frac{e^2 \bar{\Gamma}^2}{16} R_B \int \frac{d\epsilon}{2\pi} \text{Tr} (\hat{q}^{RR} + \hat{q}^{AA}) \Delta_{\epsilon-\omega/2}^{(-)} \Delta_{\epsilon+\omega/2}^{(-)} \\ S_1^K(\omega) = -\frac{1}{4} e^2 \bar{\Gamma}^2 \sqrt{R_B} \int \frac{d\epsilon}{2\pi} \text{Tr} [(\hat{q}^{RK} - \hat{q}^{KA}) \bar{n}\bar{\tau} \Delta_{\epsilon-\omega/2}^{(-)} + (\omega \rightarrow -\omega)] \quad (\text{C10})$$



$$S_1^{AA+RR}(\omega) = \frac{e^2 \bar{\Gamma}^2 \sqrt{R_B}}{4(1+x)} \int \frac{d\epsilon}{2\pi} \text{Tr} \left\{ -i\nu(\hat{q}^{RR} - \hat{q}^{AA}) \left( \Delta_{\epsilon-\omega/2}^{(-)} \Delta_{\epsilon+\omega/2}^{(-)} + \frac{1}{4}(\hat{q}^{RR} + \hat{q}^{AA}) \vec{n} \vec{\tau} \right) [\Delta_{\epsilon-\omega/2}^{(-)} \Delta_{\epsilon-\omega/2}^{(+)} + (\omega \rightarrow -\omega)] \right\}$$

$$S_1(\omega) = S_1^K(\omega) + S_1^{AA+RR}(\omega) \tag{C11}$$

where

$$\hat{q}^{ab} = G^a(\epsilon - \omega/2)G^b(\epsilon + \omega/2)$$

and  $a, b$  label the retarded, advanced or Keldysh GFs:  $a(b) = R, A, K$ . In Eq. (C10) to order  $\sqrt{x}$  we can take  $G^K(\epsilon) = i\text{Im}G^R(\epsilon)\Delta_\epsilon^{(+)}$ . The singular contribution  $S_2$  of  $S_{d2}$  that is linear in  $x$  is presented in the main text Eq. (26).

---

<sup>1</sup>A. V. Balatsky, M. Nishijima, and Y. Manassen, *Adv. Phys.* **61**, 117 (2012).  
<sup>2</sup>Y. Manassen, R. J. Hamers, J. E. Demuth, and A. J. Castellano, Jr., *Phys. Rev. Lett.* **62**, 2531 (1989).  
<sup>3</sup>Y. Manassen, E. Ter-Ovanesyan, D. Shachal, and S. Richter, *Phys. Rev. B* **48**, 4887 (1993).  
<sup>4</sup>Y. Manassen, I. Mukhopadhyay, and N. Ramesh Rao, *Phys. Rev. B* **61**, 16223 (2000).  
<sup>5</sup>C. Durkan and M. E. Welland, *Appl. Phys. Lett.* **80**, 458 (2002).  
<sup>6</sup>P. Messina, M. Mannini, A. Caneschi, D. Gatteschi, L. Sorace, P. Sigalotti, C. Sandrin, P. Pittana, and Y. Manassen, *J. Appl. Phys.* **101**, 053916 (2007).  
<sup>7</sup>M. Mannini, P. Messina, L. Sorace, L. Gorini, M. Fabriziooli, A. Caneschi, Y. Manassen, P. Sigalotti, P. Pittana, and D. Gatteschi, *Inorganica Chimica Acta* **360**, 3837 (2007).  
<sup>8</sup>V. Mugnaini, M. Fabriziooli, I. Ratera, M. Mannini, A. Caneschi, D. Gatteschi, Y. Manassen, and J. Veciana, *Sol. St. Sci.* **11**, 956 (2009).  
<sup>9</sup>T. Komeda and Y. Manassen, *Appl. Phys. Lett.* **92**, 212506 (2008).  
<sup>10</sup>Y. Sainoo, H. Isshiki, S. M. F. Shahed, T. Takaoka, and T. Komeda, *Appl. Phys. Lett.* **95**, 082504 (2009).  
<sup>11</sup>D. Mozyrsky, L. Fedichkin, S. A. Gurvitz, and G. P. Berman, *Phys. Rev. B* **66**, 161313 (2002).  
<sup>12</sup>L. N. Bulaevskii, M. Hruska, and G. Ortiz, *Phys. Rev. B* **68**, 125415 (2003).  
<sup>13</sup>S. A. Gurvitz, D. Mozyrsky, and G. P. Berman, *Phys. Rev. B* **72**, 205341 (2005).  
<sup>14</sup>M. Braun, J. König, and J. Martinek, *Phys. Rev. B* **74**, 075328 (2006).  
<sup>15</sup>O. Entin-Wohlman, Y. Imry, S. A. Gurvitz, and A. Aharony, *Phys. Rev. B* **75**, 193308 (2007).  
<sup>16</sup>A. V. Balatsky, Y. Manassen, and R. Salem, *Phil. Mag. B* **82**, 1291 (2002); *Phys. Rev. B* **66**, 195416 (2002).  
<sup>17</sup>Y. Manassen and A. V. Balatsky, *Special issue on single molecule spectroscopy: Israel Journal of Chemistry* **44**, 401 (2004), [arXiv:cond-mat/0402460](https://arxiv.org/abs/cond-mat/0402460).  
<sup>18</sup>L. S. Levitov and E. I. Rashba, *Phys. Rev. B* **67**, 115324 (2003).  
<sup>19</sup>L. Arrachea, A. Caso, and B. Horowitz, [arXiv:1305.6477](https://arxiv.org/abs/1305.6477).  
<sup>20</sup>R. López, D. Sánchez, and L. Serra, *Phys. Rev. B* **76**, 035307 (2007).  
<sup>21</sup>J. Bork, Y. Zhang, L. Diekhöner, L. Borda, P. Simon, J. Kroha, P. Wahl, and K. Kern, *Nat. Phys.* **7**, 901 (2011).  
<sup>22</sup>W. Hofstetter, J. König, and H. Schoeller, *Phys. Rev. Lett.* **87**, 156803 (2001).  
<sup>23</sup>J. S. Lim, M. Crisan, D. Sánchez, R. López, and I. Grosu, *Phys. Rev. B* **81**, 235309 (2010).  
<sup>24</sup>A. Golub and Y. Avishai, *Phys. Rev. B* **69**, 165325 (2004).  
<sup>25</sup>J. König and Y. Gefen, *Phys. Rev. B* **65**, 045316 (2002).  
<sup>26</sup>E. M. Lifshitz and L. P. Pitaevskii, *Physical Kinetics, Course of Theoretical Physics* (Pergamon Press, Oxford, 1981).  
<sup>27</sup>A. Kamenev and A. Levchenko, *Adv. Phys.* **58**, 197 (2009).  
<sup>28</sup>Ya. Blanter and M. Büttiker, *Phys. Rep.* **336**, 1 (2000).  
<sup>29</sup>Y. Meir, N. S. Wingreen, and P. A. Lee, *Phys. Rev. Lett.* **66**, 3048 (1991).  
<sup>30</sup>Z. Wilamowski, W. Jantsch, H. Malissa, and U. Rossler, *Phys. Rev. B* **66**, 195315 (2002).  
<sup>31</sup>C. Tahan and R. Joynt, *Phys. Rev. B* **71**, 075315 (2005).  
<sup>32</sup>A. M. Shikin, A. Varykhalov, G. V. Prudnikova, D. Usachev, V. K. Adamchuk, Y. Yamada, J. Riley, and O. Rader, *Phys. Rev. Lett.* **100**, 057601 (2008).  
<sup>33</sup>E. Rotenberg, J. W. Chung, and S. D. Kevan, *Phys. Rev. Lett.* **82**, 4066 (1999).  
<sup>34</sup>J. Bardeen, *Phys. Rev. Lett.* **6**, 57 (1961).  
<sup>35</sup>C. J. Chen, *Phys. Rev. B* **42**, 8841 (1990).  
<sup>36</sup>Y. Manassen, M. Averbukh, and M. Morgenstern (unpublished); Y. Manassen (private communication).